

# Compound laser modes of mutually delay-coupled semiconductor lasers: bifurcation analysis of the locking region

H. Erzgräber<sup>1,2</sup>, D. Lenstra<sup>1,3</sup>, B. Krauskopf<sup>2,1</sup>

<sup>1</sup>Natuurkunde en Sterrenkunde, Vrije Universiteit Amsterdam, The Netherlands

<sup>2</sup>Department of Engineering Mathematics, University of Bristol, UK

<sup>3</sup>COBRA Research Institute, Technische Universiteit Eindhoven, The Netherlands

*A system of two mutually delay-coupled semiconductor lasers with a small delay of 170 ps in the coupling is studied. Apart from a possible difference in their optical frequencies, we consider two identical lasers. We show the existence and stability of compound laser modes. They are the basic solutions of the system describing a frequency locked state of the coupled laser system. A characteristic detuning scenario is shown, including a sequence of mode jumps and multistability within the locking region.*

It is well known that semiconductor lasers (SLs) are very sensitive to external perturbation. In this contribution we consider two SLs, which are mutually delay-coupled via their optical fields. The time delay  $\tau_n$  naturally arises from the finite propagation time of the light from one laser to the other. This system received increasing attention, both from a fundamental point of view as well as from an application point of view [1, 2, 3, 4, 5, 6, 7]. We concentrate on the locking region, where both lasers exhibit continuous wave (CW) emission with a common frequency but possible differences in their intensities. First, the symmetrical case of zero detuning is investigated. This gives the necessary information to understand the influence of detuning, which we investigate next. Finally, we give the physical interpretation of a bifurcation analysis within the locking region by showing what would be measured in an experiment. The bifurcation diagrams are obtained by numerical continuation with DDE-BIFTOOL [8]; when supplied with an appropriate starting solutions, this software allows one to follow solutions in parameters.

We use a rate equation model for the normalized complex slowly-varying envelope of the optical fields  $E_{1,2}$  and the normalized inversions  $N_{1,2}$ . The main modeling assumption is that the coupling rate is small enough so that feedback effects can be neglected. See Ref. [2] for a detailed derivation of these equations, which in dimensionless form are:

$$\frac{dE_1}{dt} = (1 + i\alpha)N_1E_1 + \kappa e^{-i\Omega_1\tau_n}E_2(t - \tau_n), \quad (1)$$

$$\frac{dE_2}{dt} = (1 + i\alpha)N_2E_2 + \kappa e^{-i\Omega_1\tau_n}E_1(t - \tau_n) + i\delta E_2, \quad (2)$$

$$T \frac{dN_1}{dt} = P - N_1 - (1 + 2N_1)|E_1|^2, \quad (3)$$

$$T \frac{dN_2}{dt} = P - N_2 - (1 + 2N_2)|E_2|^2. \quad (4)$$

Equations (1)–(4) are written in the reference frame of laser 1. Thus the optical fields of the lasers are represented by  $E_i(t)e^{i\Omega_1 t}$ , where  $\Omega_1$  is the optical angular frequency of laser 1 operated solitarily at threshold. The time  $t$  is measured in units of the photon

lifetime. Apart from the difference in their solitary optical frequencies, the two lasers are considered to be identical.

The mutual coupling is given by the second term of Eqs. (1) and (2). It contains the coupling rate  $\kappa$ , the delay time  $\tau_n$  and the coupling phase  $C_p = \Omega_1 \tau_n$ . Here we consider the coupling phase  $C_p$  as an independent parameter, which allows us to change the interference condition between the optical fields of the lasers. The detuning between the two lasers is taken into account by the last term of (2) where  $\delta = (\Omega_2 - \Omega_1)$ , and  $\Omega_2$  is the optical angular frequency of the second laser operated solitarily at threshold.

The remaining parameters are the linewidth enhancement factor  $\alpha$ , the normalized carrier lifetime  $T$  and the pump parameter  $P$ . For all parameters we adapt the physically meaningful values  $\tau_n = 25.49$ ,  $\alpha = 2.0$ ,  $\kappa = 0.047$ ,  $T = 150.0$ , and  $P = 13.17$ .

A more detailed discussion of the properties of the model, in particular, the symmetries which are relevant to fully understand the dynamics, is beyond the scope of this paper. It can be found, for example, in [7].

The basic solution of Eqs. (1)–(4) are CW states, represented by a common optical frequency  $\omega^s$ , constant intensities  $I_i^s = |R_i^s|^2$  and inversions  $N_i^s$ , which may be different for both lasers. There is generally a phase difference  $\sigma$  between the two lasers. These solutions are called *compound laser modes* (CLMs) and can be written in the form

$$E_1(t) = R_1^s e^{i\omega^s t}, \quad E_2(t) = R_2^s e^{i\omega^s t + i\sigma}, \quad N_1(t) = N_1^s, \quad N_2(t) = N_2^s. \quad (5)$$

First, we consider the case of zero detuning. Four types of CLMs are possible as solutions of Eqs. (5); they are plotted in Fig. 1 in the  $(\omega^s, N^s)$ -plane.

In Fig. 1(a) the *constant-phase* are shown. There are *in-phase* and *anti-phase CLMs*, which are due to constructive and destructive interference between the optical fields of the two lasers, corresponding to  $\sigma = 0$  and  $\sigma = \pi$ , respectively. For constant-phase CLMs the inversions and the intensities of both lasers are equal. The in-phase and anti-phase CLMs are both born in a saddle-node bifurcation. As  $C_p$  is decreased they move along an ellipse towards the high-inversion region, where they coalesce and disappear in a second saddle-node bifurcation. The in-phase CLMs are related to the anti-phase CLMs by a  $\pi$ -translational symmetry of Eqs. (1)–(4).

In Fig. 1(b) the *intermediate-phase* CLMs are shown. There are *increasing-phase* and *decreasing-phase* CLMs. Both are born in a pitchfork bifurcation of in-phase or an anti-phase CLMs, respectively. For intermediate-phase CLMs the inversions and intensities of both lasers are not equal. In Fig. 1(b) the inversion of laser 1 lies on the upper half of an ellipse-like curve, whereas the inversion of laser 2 is on the lower half. As  $C_p$  is decreased, these CLMs move along the curve towards the high-inversion region, where they coalesce and disappear in a second pitchfork bifurcation. In this process the phase difference  $\sigma$  is no longer constant, but instead accumulates an additional phase shift of  $\pi$  as a function of  $C_p$ . The increasing-phase CLMs are related to the decreasing-phase CLMs by the same  $\pi$ -translational symmetry of Eqs. (1)–(4).

Having a comprehensive picture of the basic solutions of the system for zero detuning, we are now in a position to investigate the influence of the detuning. In Fig. 2 the CLMs are plotted in the  $(\Omega_2, I_{1,2}^s)$ -plane for two different values of the coupling phase  $C_p$ . CLMs are born and lost pairwise in saddle-node bifurcations. Since detuning destroys the reflection symmetry of Eqs. (1)–(4), the pitchfork bifurcations unfold to saddle-node bifurcations;

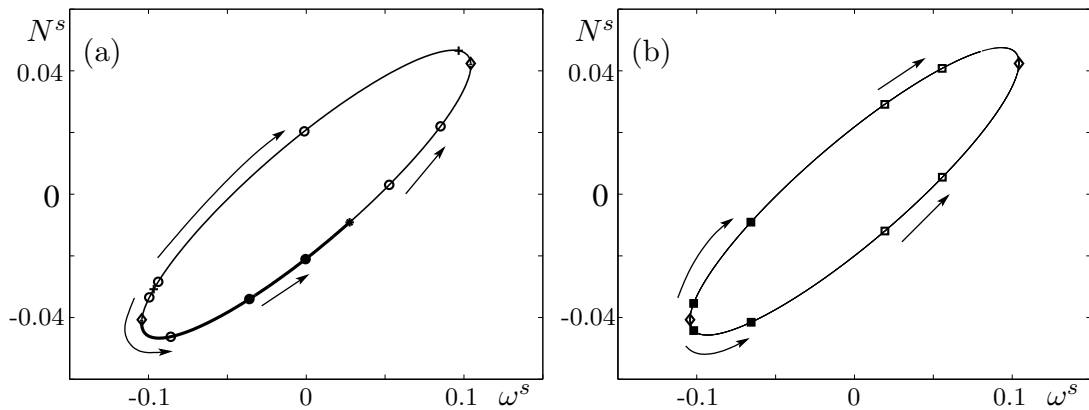


Figure 1: The constant-phase CLMs (a) and the intermediate-phase CLMs (b) for zero detuning in the  $(\omega^s, N^s)$ -plane. The arrows indicate how the CLMs move as a function of decreasing  $C_p$ . (In (a)  $C_p$  is changed from  $0.6\pi$  to  $0.2\pi$ , and in (b) from  $0.5\pi$  to  $0.2\pi$ .) Full circles denote in-phase CLMs and open circles denote anti-phase CLMs. Full squares denote increasing-phase CLMs and open squares denote decreasing-phase CLMs; saddle-node bifurcations are marked by pluses, pitchfork bifurcations by diamonds, and Hopf bifurcations by stars; stable regions are plotted as bold curves.

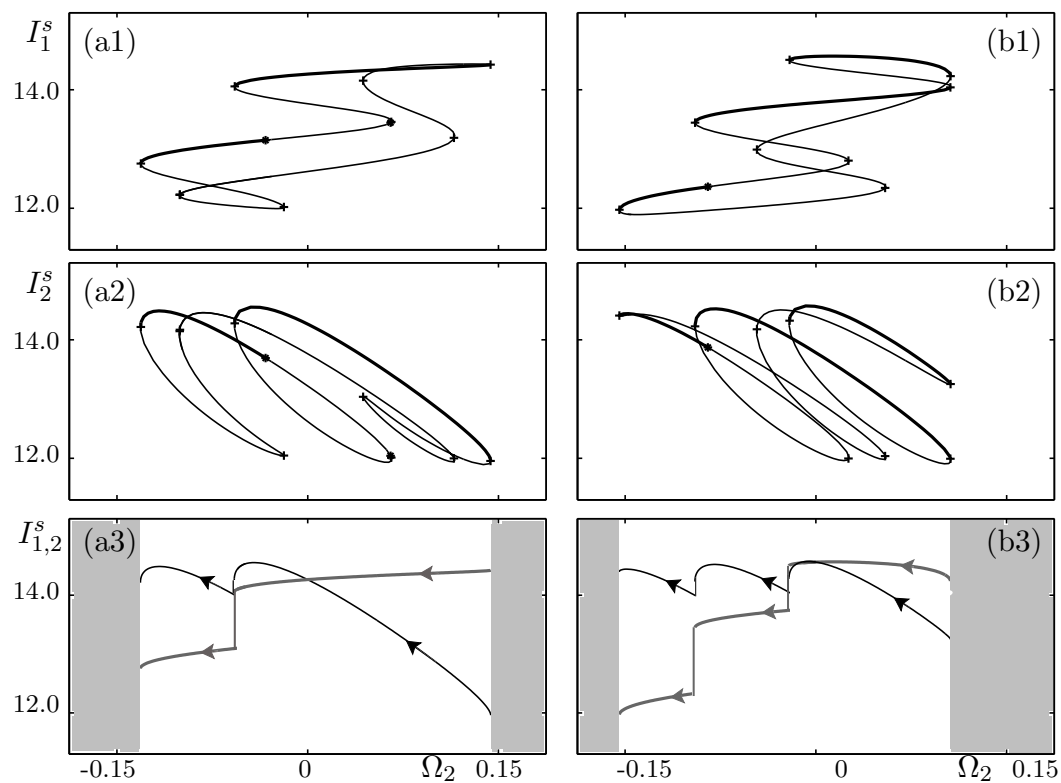


Figure 2: CLMs in the  $(\Omega_2, I_1^s)$ -plane (row 1) and in the  $(\Omega_2, I_2^s)$ -plane (row 2). Row 3 shows the parts of the stable branches that which would be observed experimentally for decreasing  $\Omega_2$ , where the intensity of laser 1 is plotted in gray and that of laser 2 in black. The gray areas are outside the locking region. Column (a) is for  $C_p = 0$  and column (b) for  $C_p = 4/6\pi$ .

## Compound laser modes of mutually delay-coupled semiconductor lasers: bifurcation analysis of the locking region

see Ref. [7] for details. Tracing the CLMs with numerical continuation results in closed, self-intersecting curves, whose exact shape depends on the value of  $C_p$ . CLMs may be stable all the way from their appearance to their disappearance or may stabilize/destabilize in Hopf bifurcations. For each value of  $C_p$  there are regions of stable CLMs, which may overlap.

To translate this bifurcation analysis to measurements one would get in an experiment we plot only the observable parts of the branches in Fig 2(a3) and (b3) for the case of decreasing the frequency  $\Omega_2$  of laser 2. The frequency of laser 1 is set to  $\Omega_1 = 0$ ; the outside of the locking region is shaded gray. Starting with a large positive detuning, the locking region is entered from the right by decreasing  $\Omega_2$ . The system hits a saddle-node bifurcation, two CLMs are born, of which one is stable. One observes that the laser with the higher solitary frequency has a lower intensity. Gradually decreasing  $\Omega_2$  results in an increase of the intensity of laser 2, whereas the intensity of laser 1 stays almost constant. At zero detuning the intensities are equal. Eventually the system hits another saddle-node bifurcation where the stable CLM disappears. Thus, a jumps to the next available stable CLM occurs, observable by an intensity drop of both lasers. Further decreasing  $\Omega_2$  results again in an intensity increase for laser 2, whereas the intensity of laser 1 is almost constant. In Fig 2(a3), for  $C_p = 0$ , this last CLM is lost in a saddle-node bifurcation and the system leaves the locking region. However, in Fig 2(a3), for  $C_p = 4/6\pi$ , there are three stable branches CLMs in the locking region. Note that the multistability of the system will result in hysteresis loops when decreasing and then increasing  $\Omega_2$ .

In conclusion, we gave a geometrical picture of the CLMs of two SLs that are mutually delay-coupled via their optical fields. From the bifurcation analysis we extracted the behavior of the lasers' intensities as it can be observed experimentally. The understanding of this basic structures is necessary for the understanding of more complicated behavior.

## References

- [1] T. Heil, I. Fischer, W. Elsässer, J. Mulet, C. R. Mirasso, "Chaos Synchronization and Spontaneous Symmetry-Breaking in Symmetrically Delay-Coupled Semiconductor Lasers", *Phys. Rev. Lett.*, vol. 86, pp. 795–798, 2001.
- [2] J. Mulet, C. Masoller, C. R. Mirasso, "Modeling Bidirectionally Coupled Single-Mode Semiconductor Lasers", *Phys. Rev. A*, vol. 65, pp. 063815, 2002.
- [3] J. Javaloyes, P. Mandel, D. Pieroux, "Dynamical properties of lasers coupled face to face", *Phys. Rev. E*, vol. 67, pp. 036201, 2003.
- [4] F. Rogister, J. García-Ojalvo, "Symmetry breaking and high-frequency periodic oscillations in mutually coupled laser diodes", *Opt. Lett.*, vol. 28, pp. 1176–1178, 2003.
- [5] S. Yanchuk, K. Schneider, L. Recke, "Dynamics of two mutually coupled semiconductor lasers: instantaneous coupling limit", *Phys. Rev. E*, vol. 69, pp. 056221, 2004.
- [6] E. A. Viktorov, A. M. Yacomotti, P. Mandel, "Semiconductor lasers coupled face-to-face", *J. Opt. B: Quantum Semiclass.*, vol. 6, pp. L9–L12, 2004.
- [7] H. Erzgräber, D. Lenstra, B. Krauskopf and I. Fischer, "Dynamical properties of mutually delayed coupled semiconductor lasers", *Proc. SPIE*, vol. 5452, pp. 352–361, 2004.
- [8] K. Engelborghs, T. Luzyanina, G. Samaey, "DDE-BIFTOOL v. 2.00 user manual: a Matlab package for bifurcation analysis of delay differential equations. Technical report TW-330.", *Department of Computer Science, K.U. Leuven*, Leuven, Belgium, 2001.